Polymers for Advanced Technologies

WILEY

polymers advanced technologies

RESEARCH ARTICLE OPEN ACCESS

Optimizing 3D-Printing Parameters for Enhanced Mechanical Properties in Liquid Crystalline Polymer Components

Chiara Battistelli[1] | Stefano Seriani[1] | Vanni Lughi[1] | Emanuele Alberto Slejko[2]

[1]Department of Engineering and Architecture, University of Trieste, Trieste, Italy | [2]CNR-IMEM, Institute of Materials for Electronics and Magnetism, National Research Council of Italy, Genova, Italy

Correspondence: Emanuele Alberto Slejko (emanuelealberto.slejko@cnr.it)

Received: 9 September 2024 | **Revised:** 30 November 2024 | **Accepted:** 4 December 2024

Funding: This research has been supported by the Italian Space Agency (ASI) under the Framework Agreement n. 2019-7-Q.0, Italian Space Agency—University of Trieste, Executive Agreement "RISE—Resilient Integrated Structural Elements."

Keywords: additive manufacturing | annealing | fused deposition modeling | interlayer adhesion

ABSTRACT

This study investigates the influence of three critical 3D-printing parameters—layer height, print speed, and extrusion temperature—on the mechanical properties of liquid crystalline polymer 3D-printed specimens, using a low-end 3D-printer. The extrusion process during 3D-printing can further align the molecular domains within the material along a common direction, leading to a reinforced polymer structure with superior properties. Specifically, the tensile strength, deformation at rupture, and flexural elastic modulus were evaluated to determine how layer height, print speed, and extrusion temperature affect the structural integrity of the printed components. The results demonstrate a significant improvement in both tensile strength and flexural modulus with the reduction of layer height from 0.16 to 0.08 mm. The study highlights the challenges associated with interlayer adhesion in liquid crystalline polymers 3D-printing, which is crucial for optimizing the mechanical performance of printed parts. Post-processing annealing was conducted over a wide temperature range (100°C–250°C), revealing its potential to further enhance material strength, though molecular diffusion emerged as a limiting factor in its effectiveness. By successfully demonstrating these advancements with a low-end 3D printer, this research paves the way for wider adoption of liquid crystalline polymers in additive manufacturing. The use of accessible and cost-effective equipment ensures that these high-performance materials can be integrated into diverse applications, promoting democratization of advanced polymer technologies.

1 | Introduction

The demand for increasingly high-performance polymers that can substitute composites or metal alloys is growing within advanced engineering sectors, such as automotive, defense, and aerospace [1–3]. However, the adoption of high-performance polymers remains limited due to their high processing costs and complexity, which pose significant barriers to their widespread use in these industries. Materials combining lightness with elevated stiffness and mechanical resistance are often needed, especially if produced by 3D-printing. Thermotropic liquid crystal polymers (TLCPs) could effectively meet these requirements thanks to their excellent mechanical properties related to the self-assembly of their rigid molecules into oriented domains during heating. Liquid Crystal Polymers (LCPs) are a class of high-performance plastic materials. In the last few decades, they have attracted increasing interest because of their extraordinary properties, such as high mechanical strength, high thermal

stability and chemical resistance, low coefficient of thermal expansion, and low gas permeability. These features derive from the rigid and anisotropic (typically rod-like) molecules constituting their chains, which can form thermodynamically stable intermediate mesophases orienting themselves along a common direction (like in solid crystals) while not maintaining positional order (like in ordinary liquids) [4–8]. Among all classes of LCPs, TLCPs are those in which intermediate liquid crystalline mesophases occur during heating; this subclass has gained more attention because they can be melted and are characterized by low viscosity and easy processability compared with other classical thermoplastic polymers [9].

Fused deposition modeling (FDM) is an additive manufacturing process that creates three-dimensional objects layer-by-layer from thermoplastic materials. During FDM, a filament spool is fed into a heated extrusion nozzle. The filament is heated to its melting point, causing it to become malleable. As the nozzle moves along a predefined path dictated by the design model, it deposits the melted filament onto a build platform one layer at a time. The material quickly cools and solidifies, forming a solid cross-section of the object. The nozzle continues to deposit filament until the entire object is created. Thanks to its simple setup and efficient processing, FDM allows for the creation of complex geometries and customizable designs at a relatively low cost and high speed compared to traditional manufacturing methods [10, 11]. FDM additive manufactured components are generally still associated with poorer mechanical properties than those obtainable with conventional fabrication methods because they are highly anisotropic and have weak interlayer bond interfaces. Consequently, transforming FDM-printed parts into functional objects, particularly for practical high-performance applications, remains a challenge [12].

Moreover, much research has been conducted on the most used polymers for 3D-printing, which are often associated with relatively poor mechanical properties, while studies on technical polymers with higher performance are, to date, very limited. This is mainly related to their complex processing requirements: one of the key challenges is the elevated processing temperatures associated to manufacturing of high-performance polymers, often higher than 300°C. As a result, these materials often require processing conditions, which may exceed the capabilities of standard FDM printers [13]. Moreover, the inherent properties of high-performance polymers, such as their high viscosity and poor melt flow characteristics, can lead to difficulties in extrusion and filament deposition during the FDM process [14].

Achieving uniform and consistent filament extrusion becomes crucial for producing high-quality parts, but the unique rheological properties of these polymers can complicate this process. Post-processing considerations such as part cooling and annealing may be necessary to alleviate residual stresses and enhance the mechanical properties of FDM-printed high-performance polymer parts [15]; optimizing these post-processing steps for specific high-performance polymers can be intricate and time-consuming [16, 17]. Difficulties in the printing process also concern LCPs but they are gaining attention in the field of additive manufacturing because of two main advantages: their low melt viscosity that, unlike other engineering polymers such as PEEK, facilitates the extrusion through the nozzle; their peculiar self-reinforcing characteristics that can emerge during FDM printing process, leading to notable mechanical properties comparable with the highest-performance lightweight composites [15]. Thus, replacing composites with equally lightweight, stiff, and strong LCPs could be desirable in some applications because filler-matrix compatibility issues, which usually take place at the interface and are strongly influenced by the adhesion between the two components, would be avoided and significant drawbacks like the difficulty in shaping and recycling could be overcome [15]. Therefore, it is worth investigating these aspects to enable the realization of not just prototypes but also load-bearing final products, which have great potential in various engineering applications such as aerospace, industrial, and biomedical fields. However, the fabrication of high-performance polymers using low-end 3D printers remains a challenge due to their limited precision, reduced thermal control, and susceptibility to defects such as poor layer adhesion and warping. Overcoming these limitations is crucial to making these materials more accessible for widespread use, as low-end printers represent a cost-effective solution that could democratize the adoption of high-performance polymers in diverse industries.

LCPs are suitable alternatives to light alloys—in terms of specific strength, stiffness, and functional properties—for advanced applications such as those in the aerospace sector. One prominent example of the importance of polymers in this sector is the production of polymeric structures of small satellites [18, 19]. Besides the advantage of a lower mass of the subsystem, which is associated with a lower cost for launching the satellite, polymers usually require less time to ablate than light alloys and metals. In fact, the enormous number of satellites to be launched in the future poses several concerns about the risk associated with potential impacts on the Earth's surface (due to incomplete ablation of these spacecraft) during their re-entry into the atmosphere at their end-of-life. Therefore, polymers approaching the performance of metals are acquiring increasing importance in the aerospace sector thanks to their lower density and the ability to demise faster during re-entry in the atmosphere; furthermore, they also allow easier formability by 3D-printing [18]. Fabrication of components with additive manufacturing opens the way to a more straightforward design of complex optimized structures and integrated parts; these characteristics are critical for the future in-orbit manufacturing of spacecraft components and exploration activities on the Moon, for example, enabling the full potential of additive manufacturing for space applications [18].

At temperatures higher than the melting temperature of the material, TLCPs have the ability to self-assemble into nematic domains (size in the range of approximately 10 μm), in which the rigid molecular chains are micro-periodically oriented [15]. Inside the FDM starting filament, the polymer structure presents multiple domains, with each domain characterized by a local director (Figure 1a). When the filament melts and passes through the printer nozzle, shear and elongational stresses align the domains along the flow extrusion direction (Figure 1b) if the residence time is short and no thermal relaxation occurs [20]. As the molten filament (raster) exits out of the nozzle, it is exposed to the ambient temperature: cooling occurs more rapidly on the surface—leading to the solidification of the aligned nematic order—while, in the hot interior

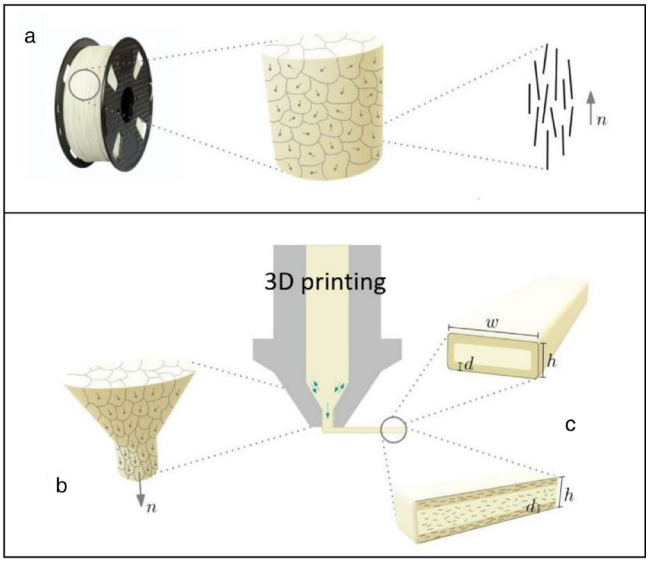

FIGURE 1 | Schematic representation of the FDM printing process of a liquid crystalline polymer. (a) Molecular alignment along the *n* director inside each domain of the starting filament. (b) Shear and elongational stresses align the domains along the extrusion direction. (c) Formation of a core-shell structure inside the printed raster.

of the filament, molecular chains have sufficient time to relax and reorient themselves driven by thermal motion, losing molecular orientation exponentially with time [21]. As a result, the extruded filament shows a core-shell structure in which rigid rod-like molecules are predominantly aligned within the shell (Figure 1c). This is in contrast with conventional thermoplastic polymers, which tend to have less oriented (i.e., amorphous) structures after exiting the printer nozzle; this behavior derives from processing taking place in the anisotropic nematic mesophase and not in the isotropic melt, contrary to conventional polymers. As the literature reports, the increase in the relative fraction of aligned molecules leads to an increase of both Young's modulus and tensile strength of the filaments along the extrusion direction, and a minimum misalignment is enough to sensibly reduce the mechanical properties [15]. The thickness of the shell depends on printing parameters such as the raster dimensions and the extrusion temperature. Decreasing nozzle diameter and layer height while printing with a temperature near the material fusion can produce faster solidification and a thicker fraction of oriented molecules forming the shell. However, when printing an entire object, not only the mechanical properties of the individual filaments must be considered, but also the adhesion between adjacent layers, which is a critical point for LCP 3D-printed components. As inter-raster and interlayer links are promoted with the increase of the extrusion temperature with respect to the material fusion one, it is evident that a compromise must be reached to guarantee both raster resistance and good adhesion between layers [15, 22].

3D-printing of LCPs is a novel research field, and the literature is not exhaustive yet; this work aims to contribute to advancing additive manufacturing technologies for high-performance polymers. Specifically, the objective of this research is to evaluate the feasibility of fabricating LCP using low-end 3D printers while ensuring acceptable mechanical and structural properties. This involves assessing whether the inherent material characteristics, such as tensile strength, elastic modulus, and deformation behavior, are adequately preserved or compromised during the printing process. Furthermore, the study aims to explore the potential for enhancing the printed polymer's performance through post-processing annealing treatments. A critical focus is placed on identifying and understanding the mechanisms driving the strengthening process during thermal treatment, particularly the effects of molecular alignment, interlayer diffusion, and crystallization. By addressing these questions, the research seeks to provide insights into the optimization of additive manufacturing processes for high-performance polymers, even with the cost-effective and accessible constraints of low-end 3D printers.

2 | Experimental

2.1 | Material and FDM Printing Setup

Liquid crystalline polymer was purchased from Fabru GmbH as a filament for 3D-printing with a diameter of 1.75 mm. The polymer is a random co-polyester based on para-hydroxybenzoic acid (p-HBA) and 2,6-hydroxynaphthoic acid (HNA), with a monomer ratio of 73/27 for HBA and HNA, respectively. The filament was preserved inside a dry box to avoid contamination of atmospheric water. A commercially available FDM printer (Creality Ender 3) was used: it was first modified to reach extrusion temperatures up to 320°C and the original build-plate was replaced with a borosilicate glass one, heated to 120°C during printing. The printer was fitted with a high-temperature extruder head capable of surpassing melting temperatures of 400°C. The material for the nozzle was changed to stainless steel, which is more corrosion and wear resistant, especially in these conditions. The temperature sensor in the melting-chamber was swapped with one compatible with values up to 500°C. An additional temperature sensor was placed on the cold-end of the extruder assembly, in order to enable monitoring for heat transfer anomalies. The filament feeder was replaced with a Redrex Dual Drive extrusion drive, equipped with counter rotating rollers; this configuration allows for considerably better grip on the filament without any added deformation, which could hinder the extrusion process. Finally, we equipped the machine with a Duet 2 Wifi (version 1.04c) to cope with the added sensing capabilities and to allow for an adequate degree of machine configuration capability. To achieve better adhesion with LCP, a thin layer of ABS slurry (solution prepared with 10 mL of acetone per gram of ABS) was placed on the printing plate. An open-source slicer (Ultimaker Cura) was used to generate G-code files. The parameters used for the printing process are shown in Table 1. Using a low-end 3D printer for fabricating advanced polymers offers significant technological advantages in terms of cost efficiency, accessibility, and flexibility. These printers reduce initial investment and maintenance costs, making them accessible for a broader range of users and applications. Their open-source nature allows for customization and experimentation with printing settings, which is often restricted in industrial-grade printers. At last, low-end printers are ideal for niche applications, small-batch production of different

TABLE 1 | Main parameters of the printing process.

Printing parameters	Value
Layer height	0.08 and 0.16 mm
Print speed	40 and 80 mm/s
Extrusion temperature	295°C and 305°C
Nozzle diameter	0.4 mm
Line width	0.4 mm
Wall thickness	0.8 mm
Infill density	100%
Infill line direction	−45°/90°/45°/90° (90° direction is parallel to the testing one in traction)
Build plate temperature	120°C

materials, and research environments where customization and iterative design are crucial.

2.2 | Design of Experiments

Three main variable printing parameters (factors) were considered: layer height, print speed, and extrusion temperature. A full factorial plan with two levels for each factor was adopted, for a total of eight experimental conditions. The chosen levels are 0.08 and 0.16 mm for layer height, 40 and 80 mm/s for print speed, and 295°C and 305°C for extrusion temperature. Three repeats were carried out for each experimental condition. This plan allows us to simultaneously analyze the effect of the three factors on the mechanical properties: a linear regression model was built to identify potential correlations between chosen printing parameters and printed specimens' mechanical properties (tensile strength, deformation at rupture, and flexural elastic modulus).

2.3 | Mechanical Tests

Tensile and flexural tests were carried out using a universal uniaxial testing machine (Shimadzu Autograph AGS-X Series) with a maximum load capacity of 10 kN. Standard dog-bone-shaped tensile test specimens (ASTM D638, Type V) were printed with a flat orientation and tested in bending and in traction. Flexural tests were carried out with a three-point bending setup, with a span of 48 mm, a displacement rate of 1.28 mm/min (ASTM D790) and a maximum deflection of 0.15 mm to avoid possible fractures. Tensile tests were performed (until rupture) using the same displacement rate, and the gauge length was set to 26.3 mm. The purpose of bending tests was to obtain an esteem of the specimens' Young's modulus; in fact, stress–strain curves resulting from tensile tests showed complex trends already in the first instants of deformation, with the consequent difficulty in distinguishing the linear elastic part. Vertically printed specimens with layers perpendicular to the applied load (55 × 3.8 × 2.9 mm) were subjected to three-point bending tests until rupture to estimate the interlayer adhesion strength. The displacement rate was set to 1.24 mm/min, and a span of 46 mm was used.

2.4 | Thermal Annealing

Heat treatment was performed on vertically printed specimens, so that the stress is mainly sustained by the interface between layers and not by the printed strands like in the horizontally printed specimens [23]. Two different groups of specimens were investigated, the first produced with the same low-end 3D printer as the previous section (Creality Ender 3HT) and the second using a different printer (Intamsys Funmat HT). The second group represents the reference for 3D printing with high-end equipment, and is used as comparison to identify the differences between annealing samples at low or high temperatures.

For the first group, the printing parameters were: layer height = 0.08 mm, print speed = 40 mm/s, extrusion temperature = 295°C. To avoid undesirable oxidation at high temperatures, a common aging process which negatively affects the properties of polymers, samples have been treated in a controlled environment. Each specimen was inserted into a glass pipette and sealed in the presence of argon atmosphere. Half of the specimens were inserted into the pipettes with some silica gel beads; the silica was expected to absorb any humidity produced during the heat treatment due to hypothesized post-condensation reactions. Subsequently, the sealed pipettes were placed in an oven for thermal annealing at 100°C for three different time intervals (1, 4, and 8 days). The treatment is expected to promote structural reorganization within the material. This, in turn, shall increase the stress transfer mechanism between adjacent macromolecules, improving the mechanical response of samples. Therefore, interlayer adhesion, toughness, and tensile behavior of annealed specimens were expected to increase [15]. Conversely from published literature [15, 22], the first group of specimens was annealed at low temperature (100°C) to investigate the modifications within the material's structure.

For the second group we used the same layer height and print speed as before. The printing temperature was set to 300°C and, as the printer is equipped with a thermal chamber, the environment temperature was no more the room one but a temperature of 80°C. For this second group, the annealing process was conducted in a tubular furnace with a constant flux of argon, and the annealing temperature was set to 250°C. The thermal treatment was conducted for two time intervals, namely 1 and 4 days.

2.5 | Characterizations

2.5.1 | X-ray Diffraction of Printed Filaments

Two-dimensional x-ray diffraction patterns of printed filaments with two different layer heights (0.04 and 0.16 mm) and of the starting filament (1.75 mm) were recorded on a single crystal diffractometer (XCalibur, Oxford Diffraction) with a molybdenum x-ray source and a graphite monochromator. The samples were mounted with the director axis perpendicular to the incident x-ray beam. The distance from the sample to the detector was set

to about 6 cm. The patterns were analyzed using the CrysAlis CCD software.

2.5.2 | Scanning Electron Microscopy

The 3D-printed sample was mounted on an aluminum stub coated with double-sided carbon tape and subsequently metallized with gold using an Emitech K550X sputter coater. The sample was analyzed using a Zeiss Gemini300 Scanning Electron Microscope. The images were collected using secondary electrons with 5 kV of acceleration voltage.

2.5.3 | Fourier-Transform Infrared Spectroscopy (FT-IR)

Attenuated total reflectance (ATR) FT-IR analysis was performed by using a Shimadzu IRSpirit QATR-S spectrophotometer with a diamond prism. Spectra from 4000 to 500 cm^{-1} were measured using the LabSolutions IR software.

2.5.4 | Thermogravimetric Analyses (TGA)

The analyses were conducted by using the instrument Netzsch STA 409EP. One heating run was performed from 20°C to 100°C or 250°C with a heating rate of 10 K/min, for a duration of 3 h. The tests were carried out in argon atmosphere.

2.5.5 | Differential Scanning Calorimetry (DSC)

A Netzsch—DSC 200 F3 Maia instrument was used to carry out the analyses. Two heating runs and one cooling run were performed between 30°C and 400°C, with a heating/cooling rate of 10 K/min. The temperature was kept constant for 2 min before starting the heating and cooling runs. Argon was used as purge gas while measuring. Aluminum crucibles were utilized, with a sample mass of 7–11 mg for each measure.

3 | Results and Discussion

3.1 | Mechanical Properties

Printed specimens' tensile strength and flexural elastic modulus were investigated to establish a correlation between mechanical properties and the three chosen printing parameters. Results from the linear regression model show that the most significant factor influencing both tensile strength and flexural elastic modulus is the layer height, while print speed and printing temperature seem to be not statistically relevant within the investigated experimental campaign. However, both the physical interpretation and the existing literature suggest that these parameters play a crucial role in the 3D-printing process of LCPs. Results of the mechanical characterization are reported in Figure 2. The decrease of the layer height from 0.16 to 0.08 mm is linked to a considerable increase in flexural elastic modulus (from 9.3 to 12 GPa, +29%) and tensile strength (from 73 to 103 MPa, +41%), coherently with what reported in the literature [15, 22]. The bonding interface evolution plays a critical role in the final strength of 3D-printed objects. High contact pressures are known for influencing the layer quality and the interlayer contact areas. Lower layer heights are therefore beneficial as, reducing the space between the nozzle and the previous layer, the higher contact pressure of the melt guarantees better adhesion between layers [24–26]. The effects of printing speed and extrusion temperature in terms of flexural modulus and tensile strength are negligible as values are within the standard deviations of the measurements (see Table S1). The strain at rupture of LCP samples is unaffected by the printing conditions investigated in this research. Previous studies have confirmed that printing with a higher nozzle temperature helps in the promotion of inter-raster and interlayer adhesion; this is mainly due to a viscosity reduction, which allows better molecular diffusion, and contributes to a longer time for extruded filaments to link each other before cooling [27, 28]. Additionally, it has been reported for LCPs that increasing the printing temperature reduces molecular orientation along the printing direction, resulting in lowered tensile strength and Young's modulus. This effect is attributed to the longer cooling times required to lock in the aligned nematic microstructure. However, this correlation is referred to specimens in which all the layers are constituted of printing lines deposited parallel to the tensile direction; in contrast, for specimens printed with lines perpendicular to the tensile direction the properties increase at increasing printing temperature, due to the dominant contribution of layer adhesion [27, 28]. For the print speed, we assume that the increase of the mechanical properties at the higher level of this factor is due to two contributions: one is the increasing shear rate of the melt, and thus a better molecular orientation in the printing direction [22]; the other is the fact that successive layers are formed after a shorter time gap compared to the layers deposited at low speed, thus the already deposited material has less time to cool down before the next layer is deposited, leading to stronger bonds and less void formation [29]. Some studies on PEEK 3D-printing have highlighted how higher printing speeds can help in reducing the extent of defects and voids in the printed layers due to the increased pressure on the extruded melt from the print nozzle [30], while slow print speeds can increase the chances of forming irregularities and defects, affecting dimensional accuracy [13, 31].

Hence, within the parameter space of the experimental plan, the best results are obtained when combining the lowest level for layer height and the highest level for both print speed and extrusion temperature, that is, when printing is conducted with the following parameters: 0.08—80 mm/s—305°C, respectively. However, wide data dispersion in both flexural elastic modulus and tensile strength is associated to these parameters; it is worth noting that this larger spread of data is also observed for the combination 0.16—80 mm/s—305°C. The observed significant variability in the results is likely attributable to the concurrent influence of print speed and extrusion temperature, particularly when both parameters are set at their highest levels. Indeed, it was noted that elevated values of these parameters are associated with an increased likelihood of undesirable phenomena during the printing process, such as the imprecise deposition of material.

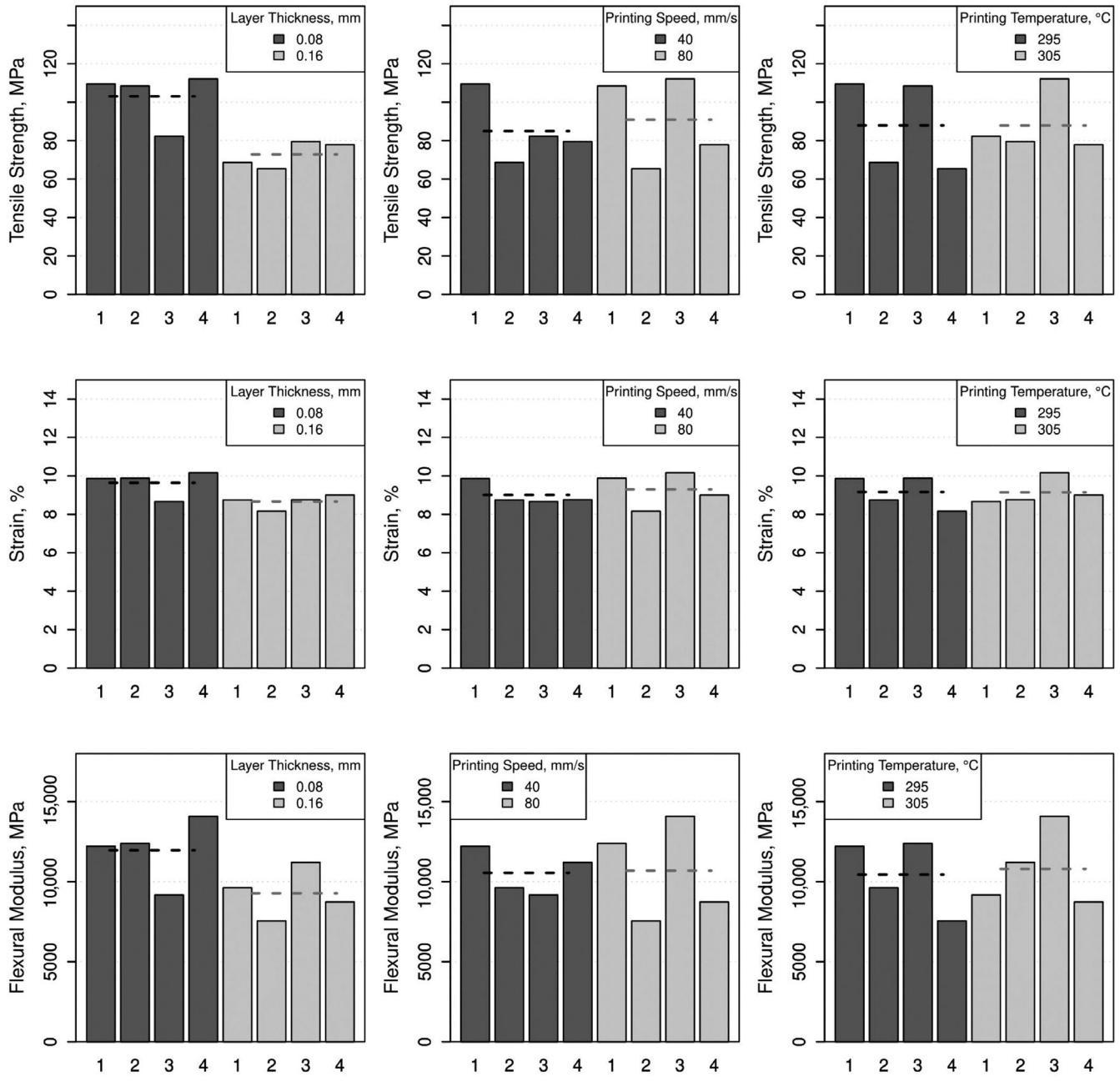

FIGURE 2 | Results of the mechanical tests on dog-bone shaped specimens; four samples have been tested for each experimental condition. Tensile strength, strain percentage, and flexural modulus for each level of the investigated factors are shown. Dashed lines indicate the mean value of the series.

The obtained results can be put in relation with the chemical–physical characteristics of LCPs 3D-printing process. It is known from the literature that lowering the layer height enhances the mechanical properties of 3D-printed parts [32, 33], and this is mainly due to the reduction of microvoids dimensions in the cross-section of the object while printing, which promotes a higher consistency and cohesion between layers. In fact, if the layer height is the same as the nozzle diameter, the cross sections of the rasters will be circular with larger voids (see Figure 3a,b); lowering the layer height will result in a flattened rectangular cross-section with round corners, and the lower the layer height, the smaller the void size [13, 23, 27, 28]. The mechanical properties and interlayer adhesion of 3D-printed LCP are strongly influenced by the thermal history experienced during the printing process, as the cooling dynamics and temperature gradients between printed layers play a critical role in determining weld times and interlayer tear energy [34]. During material extrusion, the cooling rate from the extrusion temperature to the glass transition temperature (T_g) is rapid, resulting in most layers experiencing minimal time above T_g, particularly for upper layers as the printed part grows taller. Lower layers, closer to the heated bed, maintain longer periods above T_g, benefiting from the thermal energy supplied by the bed. Increasing extrusion temperature leads to improved welding at the interface between layers, as higher road temperatures delay the cooling

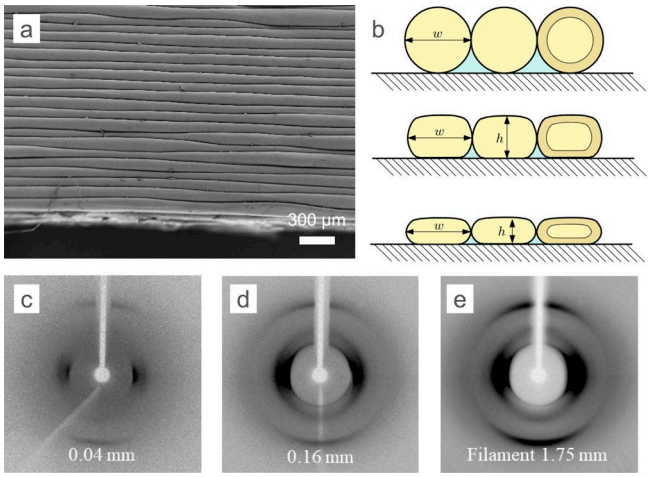

FIGURE 3 | (a) SEM image of a specimen lateral view with stacking of layers. A little over-extrusion is observed. (b) Comparison between rasters with the same width and different layer heights. Lowering the layer height reduces the size of the microvoids; moreover, the fraction of aligned skin on the cross-section of the individual rasters is higher in the thinner ones. (c–e) 2D x-ray diffraction patterns of printed filaments with different layer heights and of the starting filament; thinner samples show a higher fraction of oriented polymer.

below T_g. This results in longer weld times and enhanced mechanical properties. Similarly, higher extrusion temperatures reduce the thermal stress accumulation by improving interlayer adhesion, consistent with findings in the literature for polymers like ABS [35]. Print speed also affects the thermal behavior of LCP during printing. At higher print speeds, the time for cooling between successive layers is reduced, resulting in higher road temperatures when subsequent layers are deposited. This leads to increased tear energies due to the elevated weld time at the interface. However, increased print speed also reduces the available time for molecular diffusion, highlighting the need to balance print speed and interlayer adhesion. Finally, layer thickness influences the overall heat dissipation. Thinner layers experience a larger thermal gradient, resulting in less time above T_g and shorter weld times. This observation is supported by the trends in our experimental data, where thicker layers exhibit lower mechanical performance due to a combination of reduced contact pressure and decreased bond widths. As LCPs are highly crystalline polymers that exhibit a low fraction of free volume and very limited changes in thermal properties at temperatures close to their T_g, the impact in 3D printing these materials at temperatures below T_g may be less pronounced [36, 37]. Nevertheless, molecular dynamics and chain entanglements, being thermally activated processes, are still promoted at higher temperatures.

The observed differences in mechanical properties compared to literature data can be attributed to three main factors. First, our samples were fabricated using a modified low-end 3D printer lacking advanced features such as a heated chamber and precise control over printing parameters. This leads to suboptimal layer adhesion, uneven deposition, and an increased presence of defects such as voids and porosity, which significantly reduce the tensile strength and elastic modulus. Second, our printing strategy employed multiple line orientations to replicate real-world conditions, where stresses occur in various directions concurrently. While this approach enhances isotropy in mechanical response, it inherently sacrifices the anisotropic strength typically observed in studies utilizing unidirectional printing patterns. Finally, the higher strain at rupture observed in our samples is likely due to the increased ductility introduced by defects and voids, which promote localized deformation and crack propagation. Furthermore, the multi-line orientation contributes to a more even stress distribution during tensile loading, further enhancing the strain at rupture compared to the highly oriented structures reported in the literature.

The molecular domains of LCP orient along the extrusion direction during printing and the extruded raster show a core-shell architecture due to the different cooling rates between the surface and the interior. Consequently, thinner rasters should cool down more rapidly, preserving a higher fraction of aligned molecules in the shell. Accordingly, we have conducted a 2D x-ray diffraction analysis on samples with 0.04 and 0.08 mm thickness and on the starting LCP filament with a diameter of 1.75 mm (Figure 3c–e). All patterns obtained from the test are asymmetric, with two darker regions in the equator. Therefore, the polymer has a preferential domain orientation along the extrusion direction. Furthermore, the equatorial arcs on printed filaments are narrower than that of LCP starting filament: this indicates that the 3D-printing process improves orientation. In particular, a higher fraction of oriented polymer is present in the thinner sample, confirming that the relative fraction of highly aligned skin increases as filament thickness decreases. Hence, we assume that the mechanical properties improvement with the lower layer height arises from both the reduction of microvoids size and the presence of a higher fraction of aligned molecules in the individual rasters.

3.2 | Inter-Layer Adhesion

Accomplishing a good interlayer adhesion is particularly challenging when printing components with LCP [22]. The material has good non-sticky properties, often resulting in poor layer adhesion and components undergoing delamination while in use. This is mainly due to the anisotropic diffusion characteristic of the long rigid rod-like molecules in LCPs: considering an interface between two strands of polymer, for molecular orientation perpendicular to the interface the interdiffusion is rapid, while for molecular orientation parallel to the interface the translational diffusion is negligible [22, 38] The high degree of molecular orientation along the extrusion direction is responsible for the excellent mechanical properties of the individual LCP printed filaments. However, at the same time, it is disadvantageous for physical diffusion across the interface, resulting in very poor welding quality between layers of printed objects [22]. The effect of delamination can be observed from the stress–strain curve (Figure 4a) of tested dog-bone-shaped specimens. It can be seen how, before the complete rupture, stress drops are present; these are related to the detachment of rasters within a layer and to the delamination of adjacent layers. Thus, improving the bonding strength is fundamental to taking advantage of the LCPs full potential in terms of mechanical properties.

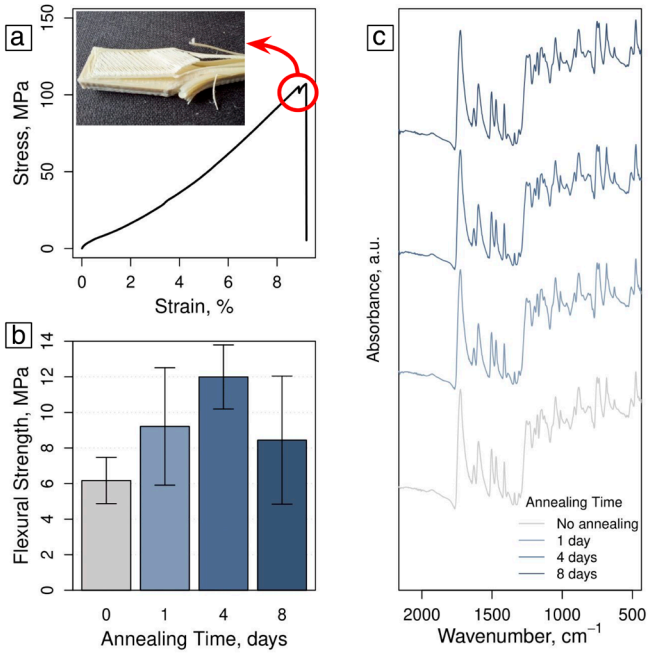

FIGURE 4 | (a) Stress–strain curve of LCP during tensile test and (inset) delamination of samples due to poor layers adhesion. (b) Improvement of the flexural strength of samples upon annealing. The increase in mechanical performance is more relevant after 4 days, then a decrease of performance is observed. (c) FTIR spectra for samples of the annealing experimental campaign.

Several techniques are used to strengthen the bond interface for FDM-printed parts, including microwave heating, infrared reheating, optimization of printing parameters, and annealing [12]. The thermal energy drives the formation of bonds among extruded material in FDM parts. The temperature history at the interfaces, influenced by printing parameters, plays a key role in determining the bonding quality and, therefore, the mechanical properties of the final product [12, 39]. Considering the parameters used in this research, we can describe their effect on the thermal history of printed parts as follows:

- Layer thickness: The amount of material extruded during the printing process affects the cooling rate of the object, as thicker layers usually require longer times to reach the same temperature than thinner layers.
- Printing speed: This parameter is related to the time required to cover the last deposited layer with a new one. Similarly, to layer thickness, the temperature of fast-deposited layers usually cools down in a slower fashion compared to slow printing speed. High printing speeds can be advantageous for the interlayer bonds strength when printing LCP because the time for effective heat dissipation decreases, that is, each layer has less time to cool before the next layer is deposited, resulting in a higher initial interface temperature and more diffusion of macromolecules on the interface [40, 41].
- Printing temperature: It is known to significantly affect bond strength, as it sets the initial temperature of the deposited filament. This, in turn, directly influences the interface temperature, which controls the diffusion of polymeric molecules across layers [40]. Moreover, with increased printing temperature the LCP molecules partly lose their parallel orientation to the interface, which also facilitates the physical entanglement between macromolecules.

Obviously, these parameters affect the thermal history of the printed object concurrently. For example, we have observed that large objects may undergo more pronounced delamination because the extrusion of new material is not fast enough to contrast the cooling of previously deposited layers. However, we have also noted that when printing with the highest print speed and the highest extrusion temperature, the distribution of measured values gets broader. These observations are in line with the literature reporting a competition between the interlayer bond strength and the dimensional accuracy and quality of the printed parts [22, 39].

3.3 | Thermal Annealing

Annealing is one of the most common post-processing methods to improve the mechanical properties of FDM-printed parts by promoting molecular diffusion across the interlayer interface and increasing crystallinity [42, 43]. The annealing time plays a vital role in the interlayer bond strength by governing the duration for viscous rearrangement and interdiffusion between neighbor layers [12].

The trend in flexural strength as a function of annealing time are reported in Figure 4b. The maximum increase is observed after 4 days, while with longer time the strength decreases. The maximum increase of flexural strength for samples is +115%, a value consistent with the results reported in the literature [15]. Gantenbein et al. highlighted how LCP printed filaments can be chemically cross-linked by thermal annealing [15]. They found that the annealing effectively increases the tensile strength, and they also suggest that the cross-linking reaction is controlled by the diffusion of reaction products (such as water molecules) away from the reaction sites. These results indicate that improving the mechanical properties of additively manufactured objects through annealing can be time-consuming, particularly for thick and large components, which adds to the overall production cost of the material. Our results indicate that annealing can be conducted even at lower temperatures; nevertheless, the final printed parts are still weaker than the ones annealed at high temperature. This challenge must be addressed in the near future to facilitate the broader adoption of LCPs in the manufacturing of high-performance 3D-printed products.

FT-IR measurements were performed before and after annealing to determine if significant chemical changes had occurred inside the material. In particular, we wanted to verify if an increase of the -CCO- band occurs as a consequence of cross-linking between LCP chains via post-condensation reactions between carboxylic acid and hydroxy groups at the end of the macromolecules. However, no significant differences can be observed from spectra reported in Figure 4c, therefore the hypothesis of post-condensation reaction happening at low temperature is discarded. In fact, this type of reactions would require encounters of functional groups in the heads and tails of LCP polymeric chains, an event very unlikely at 100°C. As the literature suggests [22, 44–46], there appear to be several

distinct processes that occur upon heating random copolyesters. Some studies state that, upon annealing at temperatures near the crystal-to-nematic transition (T_{CN}), a chemical randomization occurs through transesterification [45]. In fact, when annealing is performed at 10°C below T_{CN}, an increase of alternating copolymer sequences is expected to occur via inter-chain transesterification, thus increasing the molecular weight. For example, in Gantenbein et al., heat treatment at 10°C below T_{CN} in an inert environment results in improved tenacity and tensile properties. On the contrary, when the temperature is 40°C–50°C below, a physical reorganization of the chain into larger segregated regions is supposed to occur. The potential occurrence of chemical reactions such as transesterification during the annealing treatment at 240°C was checked by ATR-FTIR measurements in Kalfon-Cohen et al. and the aryl-ester absorbance peak observed at 1739 cm^{-1} remains unchanged after the annealing treatment, thus indicating the absence of any chemical reactions during thermal treatment at this temperature [46].

SEM micrographs of the fracture surface were collected after annealing (Figure 5). As shown, fractures occurred in the weaker sections of the samples, where uneven polymer melt coverage can be clearly observed, resulting in defects and porosity. Along the fracture surface, the presence of LCP fibrils is evident. The data suggest that the number of fibrils in the fracture area tends to decrease with increasing annealing times, supporting the hypothesis of structural reordering of the polymeric chains within the material and the formation of stronger interchain bonds.

DSC analysis conducted on annealed samples indicates the reorganization of macromolecules and rearrangement of oriented domains during thermal treatment, with the rising of more intense crystallization peaks for both series (100°C and 250°C), as reported in Figure 6a,c. These peaks are related to the increase of order within the material's microstructure caused by the improved mobility of polymer chains at high temperature. Since thermotropic LCPs are complex materials with the existence of multiple mesophases, we can observe several peaks forming during the treatment [45, 47]. In all our DSC measurements, we observe two or more endothermic peaks: the one at 273°C–277°C is assigned to the conversion of the orthorhombic structure fraction to pseudo-hexagonal arrangement, while the peak at 280°C–290°C corresponds to the crystal-to-nematic transition. The increase of the transition enthalpy with increasing annealing time is evident from our data. This is in accordance with the previous literature [45]: in fact, annealing at 40°C–70°C below the melting point (T_{CN}) leads to a significant increase in transition enthalpy with little change in the melting temperature. Diffusion processes dominate under these conditions, and it is well accepted that ordering occurs by a physical process. Within the same study, 13C NMR analyses of 73/27 HBA/HNA10 copolyesters annealed well below the T_{CN} do not indicate any change in diad sequence distribution. From DSC curves, heat of fusion for each experimental condition can be derived: trends are shown in Figure 6b,d. As can be seen from the bar plot and accordingly with the physical mechanism behind the molecular rearrangement, heat of fusion increases with annealing time, with a larger change in samples treated at 250°C. This data strongly support the hypothesis of crystallinity increase as a contributor for the improved mechanical performance of 3D-printed LCP samples. Our results suggest that chemical reaction do not occur inside the material; therefore, we suppose that, with the annealing condition employed in our study, only a physical rearrangement occurs inside the polymer, increasing the crystallinity by improving the packing between chains.

Isothermal thermogravimetric analysis conducted at 100°C and 250°C under argon atmosphere indicates that the material

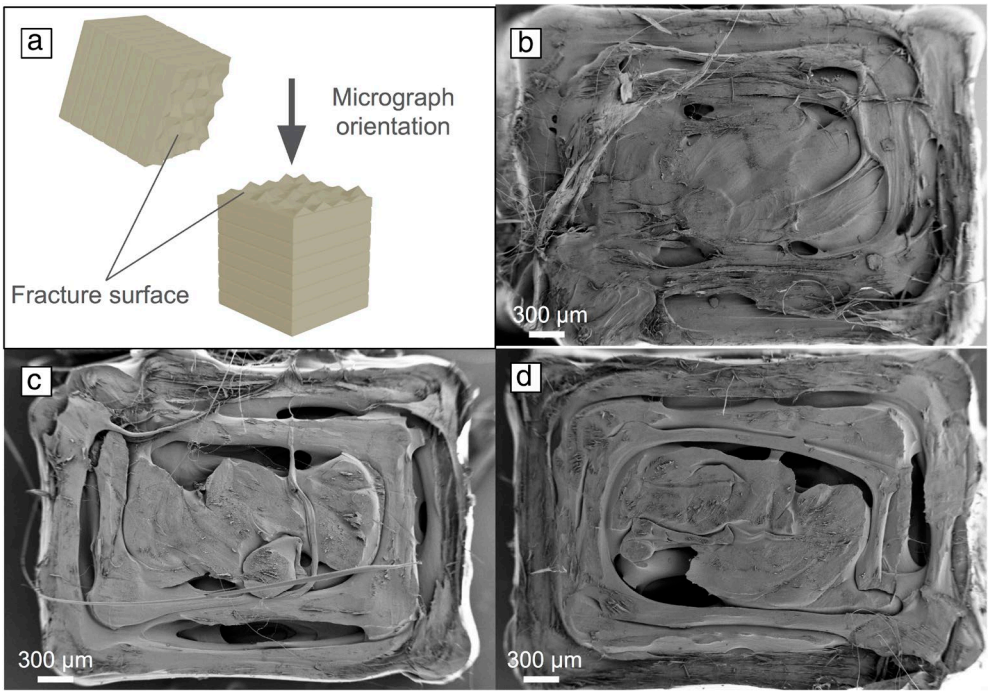

FIGURE 5 | (a) Scheme of SEM micrograph orientation on broken samples for the layer adhesion campaign. SEM micrographs of fracture interface increasing the annealing time: (b) no annealing, (c) 1-day treatment, (d) 4-day treatment.

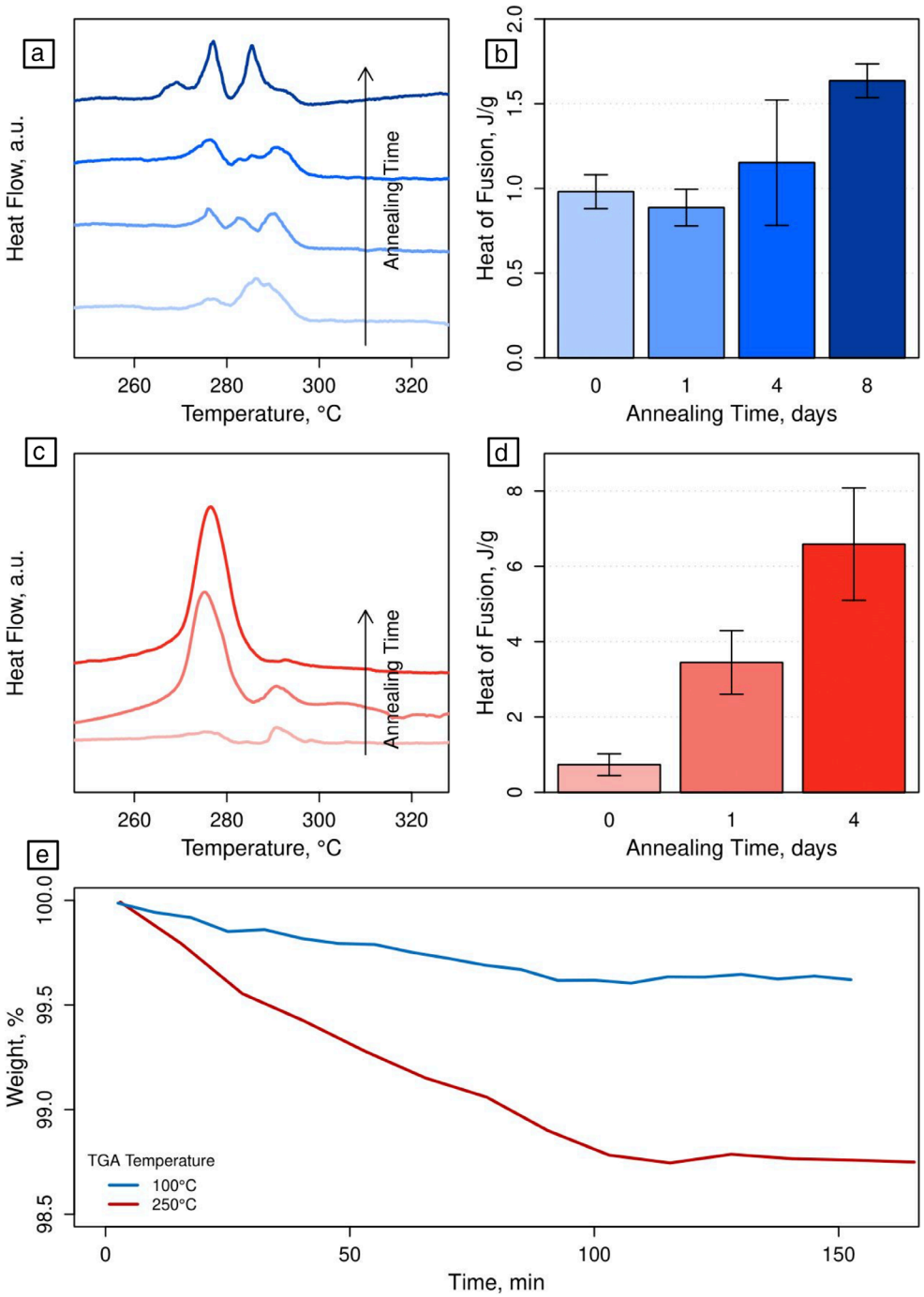

FIGURE 6 | (a) DSC curves of 3D-printed LCP samples annealed at 100°C and (b) their heat of fusion. (c) DSC curves of 3D-printed LCP samples annealed at 250°C and (b) their heat of fusion. (d) TGA results for isothermal heating at 100°C and 250°C.

releases a small percentage of its initial mass during the testing (Figure 6e). The weight reduction is in the form of small molecules and vapors, and it takes less than 150 min to complete the release. After that, the weight is stable for the rest of the testing. If we compare the total mass reduction during TGA to the amount of terminal hydrogen and hydroxyl groups in the raw material, we observe that the mass reduction is almost 10 times larger than the theoretical content of water molecules that can be formed during post-condensation (0.14% of total LCP mass). As a consequence, we believe that the reported mass loss is due to the release of volatile small molecules derived from additives inside the LCP material. It is well known that, to promote extrusion, melt flow modifiers are common addition to the composition of plastic materials [48–50]; this becomes even more important in the design and development of 3D-printer filaments. The specific nature of the released volatile molecules cannot be determined within this set of experiments. Since molecules must diffuse within the material to reach the interface and be desorbed, this process is faster at higher temperatures, as can be observed by the larger portion of weight loss for the curve at 250°C. We believe that this internal migration of small molecules favors the rearrangement of polymeric chains, as indicated by the increase in crystallinity observed in DSC curves.

3.4 | Limitations of the Present Study

The use of high-performance polymers with low-end 3D printers presents several limitations that may reduce the effectiveness of the fabrication technique. In our investigation, we observed that the low-end printer struggled to achieve the precise temperature control and mechanical stability required for processing these advanced materials, leading to a low success rate of printed samples. Additionally, the lack of efficient multi-sample printing capabilities results in significantly longer production times, as parts must be printed individually to reduce the risk of defects. This becomes even more important in terms of limited sample pool for research purposes. Furthermore, the inherent limitations of low-end printers (like, for example, the absence of a heating chamber) can lead to fabrication defects such as poor layer adhesion, which ultimately compromise the mechanical properties and overall performance of the printed parts, as discussed in the previous sections. These challenges highlight the need for optimizing both material formulations and printing parameters to bridge the gap between high-performance polymers and affordable 3D printing technologies.

4 | Conclusions

In this study, we investigated the influence of printing parameters on the mechanical properties of 3D-printed LCP components, with a specific focus on tensile strength and flexural elastic modulus. Our results demonstrated that among the various printing parameters, layer height plays a critical role in enhancing mechanical performance. A reduction in layer height from 0.16 to 0.08 mm significantly increased both the flexural elastic modulus by 29% and tensile strength by 41%. This improvement is attributed to an increase of the layer adhesion (as a result of higher contact pressure of the melt), a reduction in microvoids within the printed structure and a higher fraction of aligned molecules, especially in the outer layers of the printed filaments. Conversely, the effects of printing speed and extrusion temperature on mechanical properties were found to be minimal within the range of parameters tested, with changes remaining within the standard deviations of the measurements. However, high printing speed and high extrusion temperature led to increased variability in the mechanical properties, likely due to printing inaccuracies and imprecise material deposition. Furthermore, we observed that while the thermal history influenced by printing parameters plays a significant role in determining the bonding quality and mechanical properties of the final product, achieving good interlayer adhesion remains challenging due to the anisotropic diffusion characteristics of LCP molecules. Annealing was found to improve the mechanical properties by promoting molecular diffusion and increasing crystallinity, although the process was limited by the diffusion of small molecules. The increase of crystallinity observed in samples annealed at 250°C is higher compared to the variation observed in samples treated at 100°C, due to the thermally activated nature of the diffusion process. Our findings underline the importance of optimizing printing parameters, particularly layer height, to fully exploit the mechanical potential of LCPs in 3D-printing applications. However, the challenges associated with achieving consistent interlayer adhesion and the extended times required for effective post-processing treatments such as annealing highlight the need for further research and development. Addressing these limitations will be crucial for the broader adoption of LCPs in the manufacturing of high-performance 3D-printed products.

Acknowledgments

The authors gratefully acknowledge the assistance of Silvano Geremia in conducting the XRD measurements, Davide Porrelli for the SEM microscopies, and Paolo Fornasiero, Valentina Gombac, and Giuseppe Sportelli for their help with the annealing process. The authors would like to thank Alexandros Binios and Aurélie Hand for their valuable comments and suggestions on specific aspects of this work, which helped improve the quality and clarity of the manuscript. Open access publishing facilitated by Consiglio Nazionale delle Ricerche, as part of the Wiley - CRUI-CARE agreement.

Conflicts of Interest

The authors declare no conflicts of interest.

Data Availability Statement

The data that support the findings of this study are available from the corresponding author upon reasonable request.

References

1. A. I. Taub and A. A. Luo, "Advanced Lightweight Materials and Manufacturing Processes for Automotive Applications," *MRS Bulletin* 40 (2015): 1045–1054, https://doi.org/10.1557/mrs.2015.268.

2. S. Siengchin, "A Review on Lightweight Materials for Defence Applications: Present and Future Developments," *Defence Technology* 24 (2023): 1–17, https://doi.org/10.1016/j.dt.2023.02.025.

3. W. Zhang and J. Xu, "Advanced Lightweight Materials for Automobiles: A Review," *Materials and Design* 221 (2022): 110994, https://doi.org/10.1016/j.matdes.2022.110994.

4. V. Shibaev, "Liquid Crystalline Polymers," *Polymer Science: A Comprehensive Reference* 1 (2012): 259–285, https://doi.org/10.1016/b978-0-444-53349-4.00012-1.

5. L. Zhu and C. Y. Li, *Liquid Crystalline Polymers. Polymer Science: A Comprehensive Reference* (Cham, Switzerland: Springer, 2020), https://doi.org/10.1007/978-3-030-43350-5.

6. V. K. Thakur and M. R. Kessler, eds., *Liquid Crystalline Polymers: Volume 1—Structure and Chemistry* (Switzerland: Springer, 2016), https://doi.org/10.1007/978-3-319-22894-5.

7. V. K. Thakur and M. R. Kessler, eds., *Liquid Crystalline Polymers: Volume 2—Processing and Applications* (Cham, Switzerland: Springer, 2020), https://doi.org/10.1007/978-3-319-20270-9.

8. W. Brostow, ed., *Mechanical and Thermophysical Properties of Polymer Liquid Crystals* (Dordrecht, Netherlands: Springer Science & Business Media, 1998), https://doi.org/10.1007/978-1-4615-5799-9.

9. H. K. F. Cheng, T. Basu, N. G. Sahoo, L. Li, and S. H. Chan, "Current Advances in the Carbon Nanotube/Thermotropic Main-Chain Liquid Crystalline Polymer Nanocomposites and Their Blends," *Polymers* 4 (2012): 889–912, https://doi.org/10.3390/polym4020889.

10. T. D. Ngo, A. Kashani, G. Imbalzano, K. T. Q. Nguyen, and D. Hui, "Additive Manufacturing (3D Printing): A Review of Materials, Methods, Applications and Challenges," *Composites Part B: Engineering* 143 (2018): 172–196, https://doi.org/10.1016/j.compositesb.2018.02.012.

11. R. B. Kristiawan, F. Imaduddin, D. Ariawan, U. Ubaidillah, and Z. Arifin, "A Review on the Fused Deposition Modeling (FDM) 3D Printing: Filament Processing, Materials, and Printing Parameters," *Open Engineering* 11 (2021): 639–649, https://doi.org/10.1515/eng-2021-0063.

12. X. Gao, S. Qi, X. Kuang, Y. Su, J. Li, and D. Wang, "Fused Filament Fabrication of Polymer Materials: A Review of Interlayer Bond," *Additive Manufacturing* 37 (2021): 101658, https://doi.org/10.1016/j.addma.2020.101658.

13. P. Sikder, B. T. Challa, and S. K. Gummadi, "A Comprehensive Analysis on the Processing-Structure-Property Relationships of FDM-Based 3-D Printed Polyetheretherketone (PEEK) Structures," *Materialia* 22 (2022): 101427, https://doi.org/10.1016/j.mtla.2022.101427.

14. D. P. Simunec, J. Jacob, A. E. Z. Kandjani, A. Trinchi, and A. Sola, "Facilitating the Additive Manufacture of High-Performance Polymers Through Polymer Blending: A Review," *European Polymer Journal* 201 (2023): 112553, https://doi.org/10.1016/j.eurpolymj.2023.112553.

15. S. Gantenbein, K. Masania, W. Woigk, J. P. W. Sesseg, T. A. Tervoort, and A. R. Studart, "Three-Dimensional Printing of Hierarchical Liquid-Crystal-Polymer Structures," *Nature* 561 (2018): 226–230, https://doi.org/10.1038/s41586-018-0474-7.

16. J. R. C. Dizon, C. C. L. Gache, H. M. S. Cascolan, L. T. Cancino, and R. C. Advincula, "Post-Processing of 3D-Printed Polymers," *Technologies* 9 (2021): 61, https://doi.org/10.3390/technologies9030061.

17. F. Tamburrino, S. Barone, A. Paoli, and A. V. Razionale, "Post-Processing Treatments to Enhance Additively Manufactured Polymeric Parts: A Review," *Virtual and Physical Prototyping* 16 (2021): 221–254, https://doi.org/10.1080/17452759.2021.1917039.

18. E. A. Slejko, A. Gregorio, and V. Lughi, "Material Selection for a CubeSat Structural Bus Complying With Debris Mitigation," *Advances in Space Research* 67 (2021): 1468–1476, https://doi.org/10.1016/j.asr.2020.11.037.

19. A. Mio, F. Dogo, and E. A. Slejko, "Implementing Materials Fragmentation in the Life Cycle Assessment of Orbital Spacecraft," *Advances in Space Research* 73 (2024): 3116–3124, https://doi.org/10.1016/j.asr.2023.12.037.

20. K. S. Johann, F. Böhm, N. Kapernaum, F. Giesselmann, and C. Bonten, "Orientation of Liquid Crystalline Polymers After Filament Extrusion and After Passing Through a 3D Printer Nozzle," *ACS Applied Polymer Materials* 6 (2024): 10006–10018, https://doi.org/10.1021/acsapm.4c01921.

21. S. D. Hudson and A. J. Lovinger, "Transmission Electron Microscopic Investigation of the Morphology of a Poly(Hydroxybenzoate-Co-Hydroxynaphthoate) Liquid Crystal Polymer," *Polymer* 34 (1993): 1123–1129, https://doi.org/10.1016/0032-3861(93)90761-x.

22. K. S. Johann, A. Wolf, and C. Bonten, "Mechanical Properties of 3D-Printed Liquid Crystalline Polymers With Low and High Melting Temperatures," *Materials* 17 (2023): 152, https://doi.org/10.3390/ma17010152.

23. C.-Y. Liaw, J. W. Tolbert, L. W. Chow, and M. Guvendiren, "Interlayer Bonding Strength of 3D Printed PEEK Specimens," *Soft Matter* 17 (2021): 4775–4789, https://doi.org/10.1039/d1sm00417d.

24. T. J. Coogan and D. O. Kazmer, "Modeling of Interlayer Contact and Contact Pressure During Fused Filament Fabrication," *Journal of Rheology* 63 (2019): 655–672, https://doi.org/10.1122/1.5093033.

25. M. Zhou, X. Zhou, L. Si, et al., "Modeling of Bonding Strength for Fused Filament Fabrication Considering Bonding Interface Evolution and Molecular Diffusion," *Journal of Manufacturing Processes* 68 (2021): 1485–1494, https://doi.org/10.1016/j.jmapro.2021.06.064.

26. S. K. Kim, D. O. Kazmer, A. R. Colon, T. J. Coogan, and A. M. Peterson, "Non-Newtonian Modeling of Contact Pressure in Fused Filament Fabrication," *Journal of Rheology* 65 (2021): 27–42, https://doi.org/10.1122/8.0000052.

27. B. Akhoundi and A. H. Behravesh, "Effect of Filling Pattern on the Tensile and Flexural Mechanical Properties of FDM 3D Printed Products," *Experimental Mechanics* 59 (2019): 883–897, https://doi.org/10.1007/s11340-018-00467-y.

28. V. E. Kuznetsov, A. N. Solonin, O. D. Urzhumtsev, R. Schilling, and A. G. Tavitov, "Strength of PLA Components Fabricated With Fused Deposition Technology Using a Desktop 3D Printer as a Function of Geometrical Parameters of the Process," *Polymers* 10 (2018): 313, https://doi.org/10.3390/polym10030313.

29. A. A. Ansari and M. Kamil, "Effect of Print Speed and Extrusion Temperature on Properties of 3D Printed PLA Using Fused Deposition Modeling Process," *Materials Today Proceedings* 45 (2021): 5462–5468, https://doi.org/10.1016/j.matpr.2021.02.137.

30. H. Wu, X. Chen, S. Xu, and T. Zhao, "Evolution of Manufacturing Defects of 3D-Printed Thermoplastic Composites With Processing Parameters: A Micro-CT Analysis," *Materials* 16 (2023): 6521, https://doi.org/10.3390/ma16196521.

31. B. T. Challa, S. K. Gummadi, K. Elhattab, J. Ahlstrom, and P. Sikder, "In-House Processing of 3D Printable Polyetheretherketone (PEEK) Filaments and the Effect of Fused Deposition Modeling Parameters on 3D-Printed PEEK Structures," *International Journal of Advanced Manufacturing Technology* 121 (2022): 1675–1688, https://doi.org/10.1007/s00170-022-09360-4.

32. K. Almansoori and S. Pervaiz, "Effect of Layer Height, Print Speed and Cell Geometry on Mechanical Properties of Marble PLA Based 3D Printed Parts," *Smart Materials in Manufacturing* 1 (2023): 100023, https://doi.org/10.1016/j.smmf.2023.100023.

33. J. R. Stojković, R. Turudija, N. Vitković, et al., "An Experimental Study on the Impact of Layer Height and Annealing Parameters on the Tensile Strength and Dimensional Accuracy of FDM 3D Printed Parts," *Materials* 16 (2023): 4574, https://doi.org/10.3390/ma16134574.

34. E. A. Slejko, S. Seriani, and V. Lughi, "3D-Printed Poly(Oxymethylene): Improving Printability via PMMA Sacrificial Substrates and Characterization of the Mechanical and Thermal Properties," *Journal of Materials Research* 37 (2022): 773–783, https://doi.org/10.1557/s43578-021-00455-4.

35. A. M. Peterson and D. O. Kazmer, "Predicting Mechanical Properties of Material Extrusion Additive Manufacturing-Fabricated Structures With Limited Information," *Scientific Reports* 12 (2022): 14736, https://doi.org/10.1038/s41598-022-19053-3.

36. W. H. Jo, H. Yim, I. H. Kwon, and T. W. Son, "Thermal Properties of Thermotropic Liquid Crystalline Polymer/Polycarbonate Blends," *Polymer Journal* 24 (1992): 519–526, https://doi.org/10.1295/polymj.24.519.

37. R. K. Bharadwaj and R. H. Boyd, "Small Molecule Penetrant Diffusion in Aromatic Polyesters: A Molecular Dynamics Simulation Study," *Polymer* 40 (1999): 4229–4236, https://doi.org/10.1016/s0032-3861(98)00671-5.

38. U. S. Agarwal and R. A. Mashelkar, "Diffusion of Rigid Rodlike Molecules Across Interfaces: Implications in Welding of Liquid-Crystalline Polymers," *Macromolecules* 25 (1992): 6703–6704, https://doi.org/10.1021/ma00050a048.

39. Q. Sun, G. M. Rizvi, C. T. Bellehumeur, and P. Gu, "Effect of Processing Conditions on the Bonding Quality of FDM Polymer Filaments," *Rapid Prototyping Journal* 14 (2008): 72–80, https://doi.org/10.1108/13552540810862028.

40. T. J. Coogan and D. O. Kazmer, "Bond and Part Strength in Fused Deposition Modeling," *Rapid Prototyping Journal* 23 (2017): 414–422, https://doi.org/10.1108/rpj-03-2016-0050.

41. V. Srinivas, C. S. J. Hooy-Corstjens, and J. A. W. van Harings, "Correlating Molecular and Crystallization Dynamics to Macroscopic Fusion and Thermodynamic Stability in Fused Deposition Modeling; a Model Study on Polylactides," *Polymer* 142 (2018): 348–355, https://doi.org/10.1016/j.polymer.2018.03.063.

42. L. Cao, J. Xiao, J. K. Kim, and X. Zhang, "Effect of Post-Process Treatments on Mechanical Properties and Surface Characteristics of 3D Printed Short Glass Fiber Reinforced PLA/TPU Using the FDM Process," *CIRP Journal of Manufacturing Science and Technology* 41 (2023): 135–143, https://doi.org/10.1016/j.cirpj.2022.12.008.

43. A. C. Bruijn, G. de Gómez-Gras, and M. A. Pérez, "Thermal Annealing as a Post-Process for Additively Manufactured Ultem 9085 Parts," *Procedia Computer Science* 200 (2022): 1308–1317, https://doi.org/10.1016/j.procs.2022.01.332.

44. H. B. Kocer, I. Cerkez, and R. M. Broughton, "Annealing Studies on a Thermotropic Liquid Crystalline Polyester Meltblown Fabric," *Journal of Industrial Textiles* 46 (2017): 1656–1667, https://doi.org/10.1177/1528083716629139.

45. L. A. Schneggenburger, P. Osenar, and J. Economy, "Direct Evidence for Sequence Ordering of Random Semicrystalline Copolyesters During High-Temperature Annealing," *Macromolecules* 30 (1997): 3754–3758, https://doi.org/10.1021/ma961900w.

46. E. Kalfon-Cohen, A. Pegoretti, and G. Marom, "Annealing of Drawn Monofilaments of Liquid Crystalline Polymer Vectra/Vapor Grown Carbon Fiber Nanocomposites," *Polymer* 51 (2010): 1033–1041, https://doi.org/10.1016/j.polymer.2010.01.016.

47. L. C. Sawyer and M. Jaffe, "The Structure of Thermotropic Copolyesters," *Journal of Materials Science* 21 (1986): 1897–1913, https://doi.org/10.1007/bf00547924.

48. D. Auhl, F. Rohnstock, O. Löschke, K. Schäfer, P. Wang, and M. H. Wagner, "3D-Printing Quality in Relation to Melt Flow and Fusion Behavior of Polymer Materials," *AIP Conference Proceedings* 2107 (2019): 30004, https://doi.org/10.1063/1.5109498.

49. M. E. Mackay, "The Importance of Rheological Behavior in the Additive Manufacturing Technique Material Extrusion," *Journal of Rheology* 62 (2018): 1549–1561, https://doi.org/10.1122/1.5037687.

50. M. S. Thompson, "Current Status and Future Roles of Additives in 3D Printing—A Perspective," *Journal of Vinyl & Additive Technology* 28 (2022): 3–16, https://doi.org/10.1002/vnl.21887.

Supporting Information

Additional supporting information can be found online in the Supporting Information section.